

Article

Preliminary Study on the Removal of Steroidal Estrogens Using TiO₂-Doped PVDF Ultrafiltration Membranes

Mingquan Wang ^{1,2}, Fangshu Qu ¹, Ruibao Jia ^{2,*}, Shaohua Sun ², Guibai Li ¹ and Heng Liang ^{1,*}

¹ State Key Laboratory of Urban Water Resource and Environment, Harbin Institute of Technology, 73 Huanghe Road, Nangang District, Harbin 150090, China; wwwmq108@163.com (M.W.); qufangshu@163.com (F.Q.); liguibai@vip.163.com (G.L.)

² Institute of Water Quality Test, Urban Water Monitoring Center of Shandong Province, No. 68 Weiwu Road, Shizhong District, Jinan 250021, China; jnsunshaohua@163.com

* Correspondence: jiaruibao68@126.com (R.J.); hitliangheng@163.com (H.L.); Tel.: +86-135-053-172-93 (R.J.); +86-159-451-813-32 (H.L.)

Academic Editor: Jiangyong Hu

Received: 5 January 2016; Accepted: 28 March 2016; Published: 6 April 2016

Abstract: Steroidal estrogens are a representative type of endocrine-disrupting chemical contaminant that has been detected in surface water. In this paper, modified polyvinylidene fluoride (PVDF) membranes were prepared by adding different amounts of polyvinyl pyrrolidone (PVP) and nano-TiO₂ particles. PVDF-PVP membrane adsorption, UV photolysis and PVDF-PVP-TiO₂ membrane photocatalysis performance were investigated by considering the rejection of estrone (E1) and 17β-estradiol (E2) in the cross-flow filtration experiments. The mechanism of photocatalytic degradation on TiO₂-doped PVDF membranes was also evaluated. The results from the study indicated that adding PVP and nano-TiO₂ appropriately in PVDF membranes could be an effective method for better E1 and E2 rejection due to adsorption and photocatalytic degradation.

Keywords: steroidal estrogens; estrone; 17β-estradiol; PVDF-PVP-TiO₂ ultrafiltration membrane; photocatalysis; water

1. Introduction

Steroidal estrogens as emerging environmental endocrine disruptors have been shown to cause estrogen's biological effects on the exposed body. Human and animal waste-borne steroidal hormones, natural steroidal estrogens, belong to the group of endogenous steroidal endocrine-disrupting chemicals (EDCs), which are characterized by an estrogenic potency significantly higher (10,000 to 100,000 times) than exogenous EDCs or synthetic chemicals [1,2]. This type of material, which has stable chemical properties, is mainly produced by living organisms with a steroid class ring in the form of secretions or waste into the environment. It can cause biological accumulation *in vivo*. Estrone (E1) and 17β-estradiol (E2) examined in the present study are both typical estrogens and, in fact, have greater endocrine-disrupting activities. The disrupting activity of E2 is 1000–10,000 times greater than that of nonylphenol [3]. The hormone activity of E1, a metabolite of E2, is 0.2–0.5 times that of E2 [3]. These pollutants have potential for high risk because they can show strong biological effects, even at very low concentrations (10⁻¹²–10⁻⁹ mg/L), which could cause human body or animal reproductive dysfunction, abnormal behavior and larval mutations, *etc.* [4]. In recent years, researchers have paid much attention to such environmental estrogen effects and countermeasures. Kolpin investigated the E1 and E2 concentrations of 93 streams in the United States, finding average levels of 27 and 9 ng/L, respectively [5]. Cuong considered the surface water of the Yeongsan River and Seomjin River in Korea and found that the average concentrations of E1 ranged from 1.3 to 19.8 ng/L [6]. E1 and E2 in the

surface water of the Pearl River and Gongjiang River in southern China ranged from limit of detection (LOD) 8.2 ng/L and LOD 1.5 ng/L, respectively [7]. Lu monitored the Yellow River basin in Xi'an and found average E1 and E2 concentrations of 1980 and 1330 ng/L, respectively, in the dry season; 540 and 230 ng/L, respectively, in the normal season; and 140 and 90 ng/L, respectively, in the wet season [8]. Thus, there are steroid hormone pollution problems in different river basins and water systems throughout the world. The presence of steroidal estrogen compounds in water environments leads to the necessity of developing effective treatment techniques, either as a supplement for drinking water treatment systems to prevent the potential risk to human health or for treatment processes for municipal wastewater sludge and animal manure.

Steroidal estrogen removal methods include the membrane process, advanced oxidation, adsorption, biological methods, *etc.* [9]. Snyder used different membranes to remove 36 types of pharmaceutical and personal care products (PPCPs) and EDCs in water; the results showed that microfiltration and ultrafiltration had a certain effect on the removal rate of steroidal estrogens, but the removal rate was not high enough [10]. Ohko investigated E2 degradation via photocatalysis using TiO₂ as a slurry system, but it had disadvantages compared to the immobilized systems as the TiO₂ must be removed afterwards [11]. Not surprisingly, each removal option has advantages and limitations, and it is essential to adapt these options to the removal application. The technological development of ultrafiltration membrane modification provides a new approach to fixed TiO₂ photocatalysts [12,13]. We can manufacture a nano-TiO₂ immobilized in an ultrafiltration membrane and use this type of membrane to remove steroidal estrogens under UV photocatalysis. This approach may couple with membrane filtration and photocatalytic degradation during the reaction and probably enhance the contaminant removal efficiency. In the meantime, the problem of recycling and reusing nanomaterials can also be solved to reduce the risk of nano-material environmental pollution.

This study developed a type of polyvinylidene fluoride (PVDF)—polyvinylpyrrolidone (PVP)-TiO₂ nano-inorganic modified ultrafiltration membrane via a blending method to fix nanomaterials in the modified membrane. This new modified ultrafiltration membrane with adsorption and catalytic performance can not only improve the effect of the ultrafiltration membrane for the removal of steroidal estrogen but it can also provide a new technology to solve the problems of recycling nanomaterials. We studied the effect of the PVDF-PVP membrane, UV photolysis and the PVDF-PVP-TiO₂ membrane on the removal of E1 and E2 from water and described the PVDF-PVP-TiO₂ membrane reaction mechanism via a reaction kinetics model.

2. Materials and Methods

2.1. Chemicals

All materials were in high purity and used as received. PVDF (FR-904) was supplied by Shanghai 3F New Material Chemical Industrial Co. (Shanghai, China) PVP (PVP-K30, P95%), *N,N*-dimethyl acetamide (DMAc, 99%) and BSA were obtained from Sinopharm Chemical Reagent Co. Ltd. (Shanghai, China) nano-TiO₂ (P25, 99.8%) was produced by Aladdin Chemistry Co. Ltd. (Shanghai, China) and the target chemical standards estrone (E1, purity: 99.5%) and 17- β -estradiol (E2, purity: 99.5%) were obtained from Dr. Ehrenstorfer (Gesellschaft Mit Beschraenkter Haftung, Augsburg, Germany). Solvents used for extraction and instrumental analysis were chromatographically pure grade and obtained from Merck Cooperation (Shanghai, China). Deionized water (18.2 M Ω -cm) was sourced from a laboratory Milli-Q water purification system (Milli-Q A10, Millipore, Boston, MA, USA).

2.2. Membranes

Two kinds of composite PVDF membranes were prepared by the phase inversion process (PIP) method. Casting solutions were made in DMAc solvent, which included concentrations of PVDF (18 wt %), PVP (2 wt %) and TiO₂ (1 wt % or 0 wt %) additives with an average size of 5–10 nm in a water

bath temperature of 80 °C mixing for 8 h and then allowed to stand for 24 h for deaeration treatment. The casting solution was cast on a film applicator (Jiangsu Shengken Co. Ltd., Jiangsu, China) at 0.8 m/min with a casting knife of 200 µm space. Next, the membrane was immediately immersed in a deionized (DI) water coagulation bath at room temperature for one day at room temperature to remove the remaining solvent from the membrane structure. The PVDF-PVP membrane and PVDF-PVP-TiO₂ membrane were cleaned with DI water for use.

2.3. Cross-Flow Experiment

Cross-flow ultrafiltration coupled with photocatalysis was conducted in a laboratory-scale custom-made filtration unit. In this unit, E1 and E2 solutions were held in a 5 L brown glass bottle and fed to the membrane cell by a pump (when we performed a UV photolysis experiment, there was no membrane used). The permeation was returned back to the bottle to keep the feed concentration constant. The operation pressure was 0.1 MPa, cross-flow rate was 30 L/h, and the effective membrane area was 40 cm² (8 cm × 5 cm). A 100 W ultraviolet lamp was embedded in the cross-flow filtration unit; the membrane surface was irradiated by the lamp. The peak wavelength of UV lamp was 365 nm, and the light intensity at membrane surface was 2.5 mW/cm² (when we performed the PVDF-PVP ultrafiltration membrane adsorption test, the lamp did not work). The schematic diagram of cross-flow experiment is shown in Figure 1. The PVDF-PVP membrane was only used to perform a cross-flow experiment without the UV lamp, and the PVDF-PVP-TiO₂ membrane was used to perform a cross-flow experiment with the UV lamp; in addition, we performed the UV photolysis without a membrane. For all of the experiments, 200 mL water samples were collected every 6 min to detect residual concentration of the target, and the initial concentrations of both E1 and E2 were 200 µg/L. All of the experiments were performed at room temperature (20 °C). We did blank test with 200 µg/L E1 and E2 mixed solution run by the cross-flow experiment without UV light or membrane for 120 min, and the concentrations of E1 and E2 basically remain unchanged.

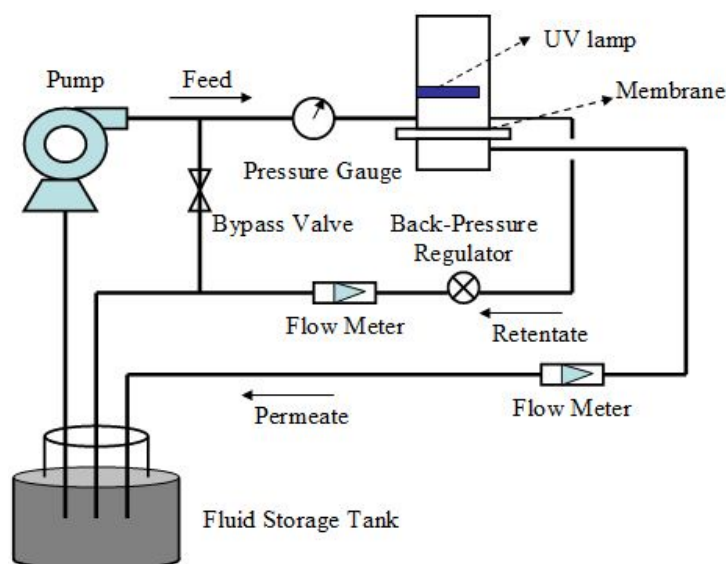


Figure 1. Schematic diagram of the cross-flow experiment.

2.4. Quantification

E1 and E2 of solution samples were analyzed on an Agilent LC-MS/MS system composed of an Agilent1100 liquid chromatograph and a QQQ6410B triple quadrupole mass spectrometer equipped with an electrospray ionization (ESI) source. Oasis hydrophile-lipophile balance (HLB) solid-phase extraction columns (Waters Corporation, Milford, MA, USA) were conditioned by pumping 6 mL methanol and 6 mL ultrapure water at a rate of 2 mL/min. Previous to sample-loading, 1000 mL

of water samples was adjusted to pH of 5.0 ± 0.5 by H_2SO_4 , and then pumped through the syringe at a flow rate of 10 mL/min. To elute columns by 10 mL ultrapure water and dry under nitrogen, then with 10 mL methylene chloride-acetone (7:3) elution. The extraction was concentrated to dry under nitrogen, and constant volume with 1 mL acetonitrile-water (3:2), under test. Analyses were performed at 40 °C in a C18 reverse-phase column (5 μm , 4.6 mm \times 250 mm, Agilent, Santa Clara, CA, USA) with 20 μL sample injections. Acetonitrile and deionized water were used as the mobile phase at a flow rate of 0.2 mL/min. The MS conditions were as follows: nebulizer pressure, 45 psi; drying gas (N_2) flow rate, 12 L/min; drying gas temperature, 350 °C; scanned area, 50–500 m/z . The retention time of E1 was determined as 2.591 min, and E2 was 2.190 min. The method had limit quantifications of E1 and E2 of 5×10^{-7} mg/L and 5×10^{-6} mg/L under this condition, respectively. The rates of E1 and E2 recovery from sextuplicate measurements were in the ranges of 75.4%–91.1% and 103.2%–120.2%, respectively, and the relative standard deviation (RSD) values were 6.6% and 7.2%, respectively, within the concentration range tested. Linear calibration curves of E1 and E2 ($R = 0.998$ and 0.996 , respectively) were established using a series of standard solutions with the lowest concentrations of 5×10^{-7} mg/L and 5×10^{-6} mg/L, respectively, and linearity ranges of 0.5–8 $\mu\text{g/L}$ and 5–80 $\mu\text{g/L}$, respectively.

The residual titanium in the solution was diluted in 1 vol % HNO_3 and determined with ICP-MS (NexIon 300 \times , Perkin Elmer, San Jose, CA, USA). Calibration curves of metal ions were constructed from 0, 1, 5, 10, 50, and 100 $\mu\text{g/L}$ of each metal ion in 1 vol % of concentrated HNO_3 in ultrapure water ($R^2 > 0.9999$).

3. Results and Discussion

3.1. Characterization of Composite PVDF Membranes

Figure 2 showed SEM images of composite PVDF membranes. These images clearly indicated that, under the same PVDF and PVP content, there were more large pores formed in the membrane surface after adding nano- TiO_2 , and the membrane pores of the cross-section became wider after the addition of nano- TiO_2 ; this probably led to the increased membrane permeation flux of the PVDF-PVP- TiO_2 membrane.

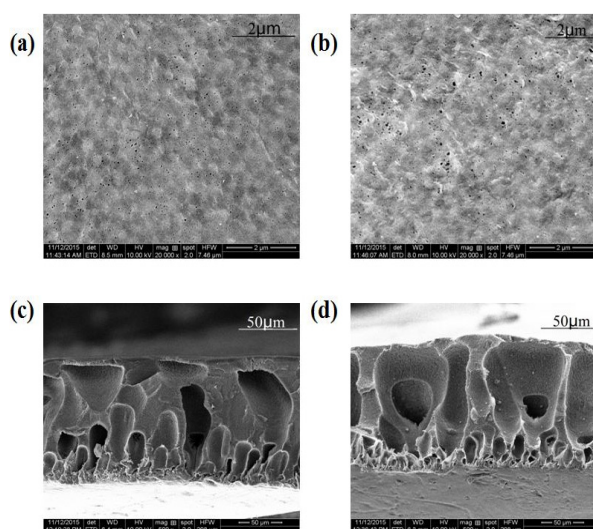


Figure 2. SEM images of composite PVDF membranes: (a) surface of PVDF-PVP membrane 20,000 \times ; (b) surface of PVDF-PVP- TiO_2 membrane 20,000 \times ; (c) cross-section of PVDF-PVP membrane 500 \times ; (d) cross-section of PVDF-PVP- TiO_2 membrane 500 \times .

Figure 3 shows the Energy Dispersive Spectrometer (EDS, INCA Energy 3294, Oxford Instrument Company, Oxford, UK) line-scan results of the PVDF-PVP- TiO_2 membranes. A small amount of

Ti was observed on the PVDF-PVP-TiO₂ membrane surface, which proved that TiO₂ nanoparticles were effectively attached to the membrane surface. The EDS surface scan also showed that TiO₂ nanoparticles were uniformly distributed on the membrane surface in the study of the membrane prepared by using PVP as an additive.

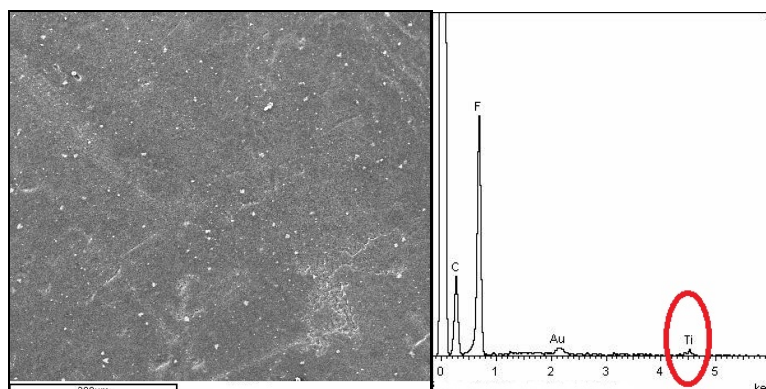


Figure 3. The elements and their contents on the PVDF-PVP-TiO₂ membrane determined by EDS.

The membrane (active area: 15.9 cm²) was placed in a dead-end stirred filtration cell (Stirred Ultrafiltration Cells, Model 8050, Millipore), which was connected to an N₂ gas supply (self-built). Under a pressure of 0.1 MPa for 30 min, DI water was used to preload the PVDF-PVP membrane and the PVDF-PVP-TiO₂ membrane. A solution containing 100 mg/L of bovine serum albumin (BSA) in DI water was used to test the membrane on its BSA permeation flux; the PVDF-PVP membrane permeation flux was 324.14 L/(m²·h), the BSA rejection rate was 53.57%; the PVDF-PVP-TiO₂ membrane permeation flux was 453.81 L/(m²·h), the BSA rejection rate was 60.54%. The PVDF-PVP-TiO₂ membrane permeation flux and rejection rate were better than those of the PVDF-PVP membrane. That is because more finger-like macro-void structures formed when nano-TiO₂ was added (Figure 2c,d) and this may enhance the membrane permeability. Li *et al.* [14] modified the PVDF hollow fiber membrane by adding TiO₂ into the casting solution, and they found that BSA permeation flux and rejection were significantly enhanced. They considered that the surface of TiO₂ was abundant with hydroxyl which could enhance the flux of PVDF membrane remarkably.

3.2. Removal Efficiencies of E1 and E2 Under UV Photolysis

Figure 4 shows the removal rates of E1 and E2 by individual UV photolysis. It was found that the apparent concentrations of E1 and E2 decreased in aqueous solutions after irradiation with the UV lamp. The degradation of E1 and E2 under UV irradiation reached equilibrium at about 100 min, and the rejection rates were 90.5% and 28.2%, respectively, at an initial concentration of 200 μg/L. The result implied that photolysis of E1 and E2 occurred in water, and E1 was easier to remove than E2. Estrogens have been reported to be amenable to transformation during UV treatment, with the light absorption attributed to the photoactive phenolic group [15,16], *i.e.*, the photolysis producing compounds containing carbonyl groups [16]. Coleman *et al.* used a recombinant estrogen assay based in yeast to follow the estrogenic activity of aqueous solutions (C_{est} of 10 μg·L⁻¹) of E1 and E2 after UVA photolysis, being most effective on E1, followed by E2 [15]. Ma *et al.* studied the removal of three co-existing steroid estrogens, estrone (E1), 17β-estradiol (E2) and 17α-ethinyl estradiol (EE2), from aqueous solutions; when the ultraviolet irradiation intensity was 168 μW/cm² and the reaction time was 120 min, the E1 removal rate was 98.1%, and the removal rate of E2 was 37.0%. Our results are consistent with the other results in the literature [17].

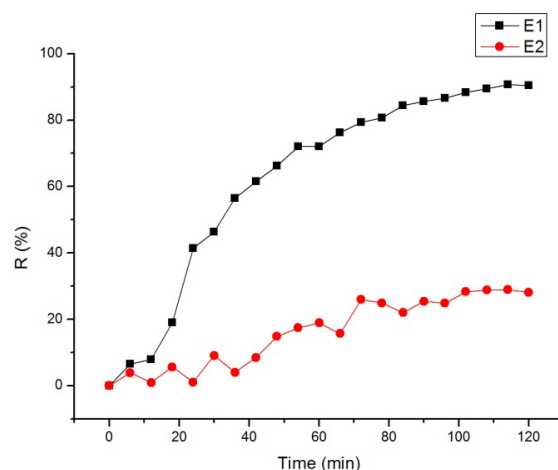


Figure 4. Removal efficiencies of E1 and E2 under UV photolysis.

3.3. Removal Efficiency of E1 and E2 Using the PVDF-PVP Ultrafiltration Membrane

Figure 5 shows the removal efficiencies of E1 and E2 by the PVDF-PVP ultrafiltration membrane under cross-flow filtration. The removal efficiencies of E1 and E2 were 33.9% and 8.0% at 120 min without irradiation of the UV lamp, and it was also shown that the removal efficiencies of E1 and E2 decreased over time. The reason E1 rejection is higher than E2 rejection is due to the octanol-water partition coefficient of the materials. Yoon *et al.* [18,19] studied the removal of EDCs (including E1 and E2) from water by ultrafiltration membranes, and the result showed that the E1 and E2 average retention rates were about 44% and 5%, respectively, using four waters spiked with EDCs, which were comparable to the rejection rates found in the current study. The probable mechanism for EDC rejection by ultrafiltration membranes is hydrophobic adsorption. He also observed visually that the retention increases with increasing the $\text{Log}K_{ow}$ value. This indicates that retention for the hydrophobic membranes is influenced by hydrophobic interaction (adsorption). By measuring the contact angle of the PVDF-PVP membrane, the membrane was found to be of relatively high hydrophobicity with a contact angle of 87° . Hence, the hydrophobic solutes such as E1 and E2 can easily migrate towards and adhere to the membrane surface, because the adhesion of water molecules to the membrane surface was quite weak due to the lack of hydrogen bonds. As a result, the ultrafiltration membrane could reject parts of E1 and E2, although its molecular weight cut-off (50 KDa) was much higher than the molecular weight of the target pollutants (E1: 270 Da, E2: 272 Da). As time increased, the membrane adsorption gradually reached saturation, leading to the decrease of E1 and E2 rejection rates. At the same time, the high cross-flow filtration pressure and long hydraulic retention time may also contribute to the low rejection rates of E1 and E2 by the ultrafiltration membrane. Adsorption under cross-flow filtration belonged to dynamic adsorption with a bad contact with aqueous solution, and it is hard to form multilayer adsorption on the membrane surface due to the hydrodynamic shear stress. Figure 5 also shows that the removal efficiencies of E1 and E2 under UV photolysis were 89.8% and 28.3% at 120 min under irradiation of the UV lamp, respectively. We can find that the results were the same as E1 and E2 removal efficiencies under UV photolysis, so under the condition of photolysis, UV light catalysis played a decisive role in the process of the PVDF-PVP ultrafiltration membrane removing the E1 and E2.

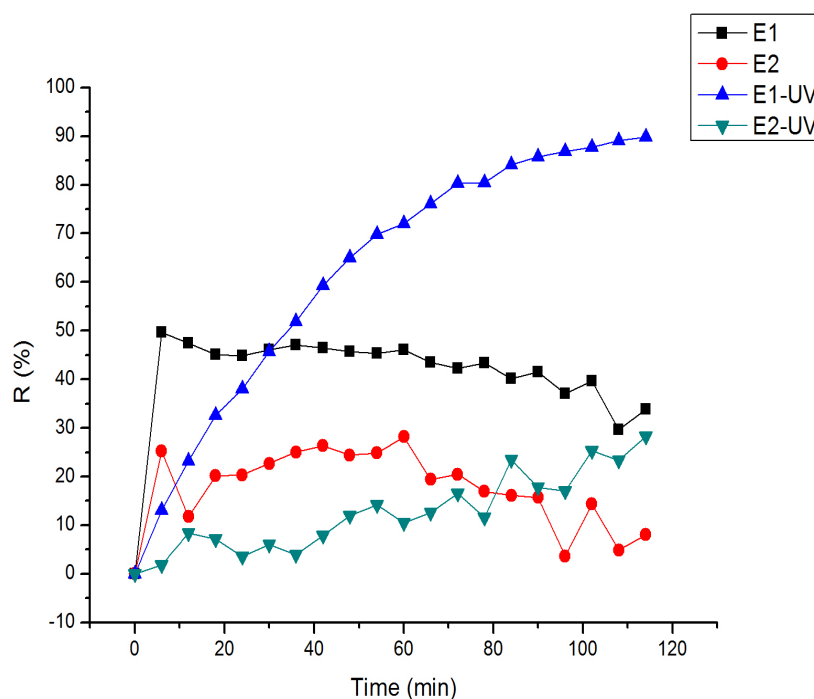


Figure 5. Removal efficiencies of E1 and E2 using a PVDF-PVP ultrafiltration membrane.

3.4. Removal Efficiencies of E1 and E2 Using the PVDF-PVP-TiO₂ Ultrafiltration Membrane

Figure 6 shows the removal efficiencies of E1 and E2 by the PVDF-PVP-TiO₂ ultrafiltration membrane. The removal efficiencies of E1 and E2 were 36.1% and 11.4% at 120 min without UV photocatalysis which was better than that by the PVDF-PVP ultrafiltration membrane. At the same time, we found that the PVDF-PVP membrane had better removal efficiencies of E1 and E2 than the PVDF-PVP-TiO₂ membrane at the beginning of the reaction. It was caused by the nano-TiO₂ addition, which improved the membrane hydrophilic and anti-pollution capacity. Under UV photocatalysis, the removal efficiencies of E1 and E2 by the PVDF-PVP-TiO₂ ultrafiltration membrane were better than those by the PVDF-PVP membrane with UV photolysis. The removal of E1 and E2 onto the PVDF-PVP-TiO₂ membrane all reached equilibrium at approximately 90 min, and the removal efficiency was approximately 93.4% and 73.1%, respectively. For both estrogens, 50% quantities were removed by photocatalysis within 30 min. The result showed that the nano-TiO₂ addition can improve the estrogen removal rate under UV irradiation effectively. Coleman *et al.* also showed that photocatalysis over TiO₂ was more effective than direct photolysis at removing the estrogenic activity of E1 and E2 (initial concentrations of 10 µg·L⁻¹) from aqueous solutions [15]. At the same time, the content of titanium in water was tested by ICP-MS, and there was none detected at the experiment.

Figure 7 shows the variations of the normalized permeate flux *versus* time for the PVDF-PVP-TiO₂ ultrafiltration membrane under darkness and UV irradiation conditions. It indicated that, under UV photocatalysis, the PVDF-PVP-TiO₂ membrane had better membrane-specific flux for long periods of time. The UV irradiation during filtration successfully improved membrane water permeability and reduced the membrane fouling. This conclusion was in accordance with the research results of Méricq *et al.* [20].

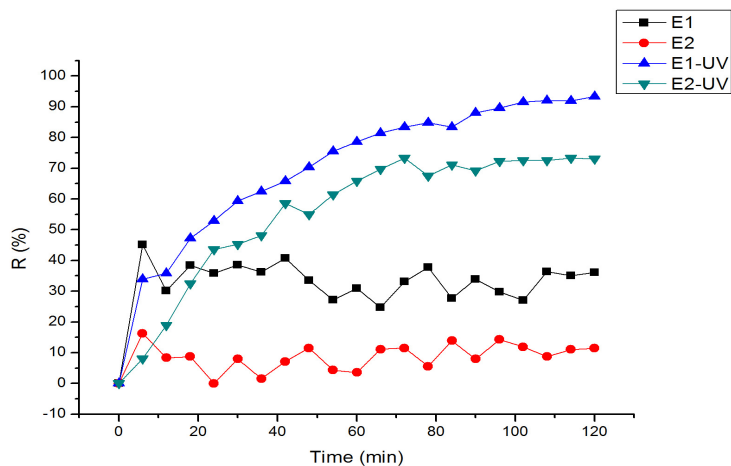


Figure 6. Removal efficiencies of E1 and E2 using the PVDF-PVP-TiO₂ ultrafiltration membrane.

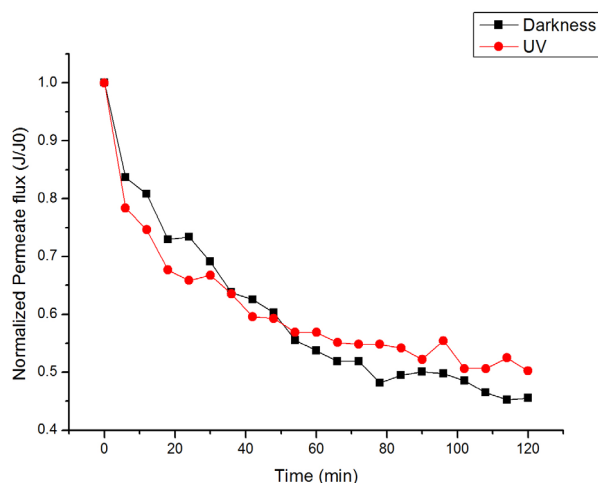


Figure 7. Normalized permeate flux (J/J_0) versus time with and without UV for PVDF-PVP-TiO₂ ultrafiltration membrane.

Based on the preliminary experimental results, it can be concluded that E1 and E2 removal using the PVDF-PVP-TiO₂ ultrafiltration membrane together with UV irradiation may be a combination of membrane adsorption and UV photolysis. Firstly, the membrane adsorption may contribute to the removal of the target pollutants, as shown in the scenario of the individual PVDF-PVP-TiO₂ ultrafiltration membrane filtration. When nano-TiO₂ was added to the PVDF-PVP membrane, the contact angle became 69°, *i.e.*, 18° lower than that of the PVDF-PVP membrane. This result showed that the hydrophilic ability of the membrane was enhanced, as was the ability of adsorption. At the same time, the result proved that E1 and E2 removal mainly depended on photocatalysis. Second, the removal might be caused by TiO₂ in the modified ultrafiltration membrane under UV irradiation. When a photon of light of sufficient energy ($E > E_{bg}$) strikes a TiO₂ particle, the energy of the photon is absorbed and used to promote an electron (e⁻) from the valence band to the conduction band. This movement of an electron leaves a hole (h⁺) in the valence band. These species (h⁺ and e⁻) produced by the absorption of light can either recombine or migrate to the surface of the TiO₂ particle, where they can react with other species at the interface. The holes can directly oxidize organic species adsorbed onto the TiO₂ particle or can give rise to hydroxyl radicals (OH) by reacting with water or OH⁻. These highly reactive hydroxyl radicals then attack organic compounds present at or near the surface. This process finally results in the formation of carbon dioxide and water, if the reaction proceeds to completion [21,22].

3.5. Photocatalytic Degradation Kinetics Analysis

The photocatalytic degradation kinetics data of E1 and E2 were analyzed by testing the first-order kinetic model and the second-order kinetic model [23] (Figure 8). The results were calculated as shown in Table 1.

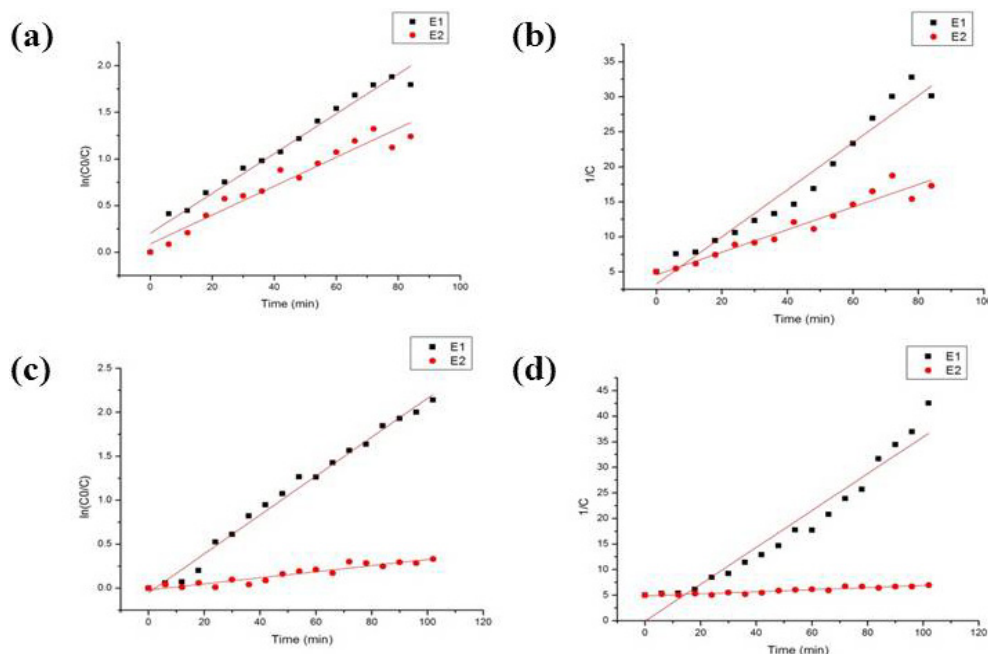


Figure 8. First-order kinetics (a) and second-order kinetics (b) fit of E1 and E2 removal on PVDF-PVP-TiO₂ membrane under UV photocatalysis; first-order kinetics (c) and second-order kinetics (d) fit of UV photolysis.

Table 1. Constants and correlation coefficients for the kinetic models.

Condition	Substance	First-Order Kinetics			Second-Order Kinetics	
		Equation	K/min ⁻¹	R ²	Equation	R ²
PVDF-PVP-TiO ₂ membrane under UV photocatalysis	E1	$\ln(C_0/C) = 0.021t + 0.204$	0.021	0.975	$1/C = 0.337t + 3.258$	0.954
	E2	$\ln(C_0/C) = 0.016t + 0.089$	0.016	0.943	$1/C = 0.162t + 4.568$	0.940
UV photolysis	E1	$\ln(C_0/C) = 0.021t - 0.052$	0.021	0.989	$1/C = 0.360t - 0.055$	0.943
	E2	$\ln(C_0/C) = 0.0035t - 0.019$	0.0035	0.908	$1/C = 0.020t + 4.850$	0.906

The measured kinetics data of E1 and E2 removed via the PVDF-PVP-TiO₂ membrane photocatalysis and UV photolysis all were fit well by the first-order model (Figure 8a,c) with a better correlation coefficient. The reaction rate constant of E1 under the condition of the PVDF-PVP-TiO₂ membrane with UV photocatalysis was the same as that of UV photolysis, and the reaction rate constant of E2 under the condition of the PVDF-PVP-TiO₂ membrane with UV photocatalysis was 4.6 times faster than UV photolysis. When nano-TiO₂ was added in the reaction system, it increased the reaction rate of E2, obviously. Besides, the concentrations of E1 and E2 were eliminated during photocatalysis, whereas variable removal rates of estrogenic activity occurred by PVDF-PVP-TiO₂ membrane photolysis, with the order E1 > E2. It could be seen that the rate for the photocatalysis of E1 was 1.3 times faster than that of E2. E1 appeared to be a less stable molecule than E2 under photocatalytic conditions. The addition of the carbonyl group may cause the molecule to be less stable and degrade easier under these conditions due to the double bond of the carbonyl group, which strongly absorbs UV light. The 17 β -estradiol appeared to degrade at a slower rate [21,24]. The addition of the OH group stabilized the phenolic ring and resisted breakdown via photocatalysis and UV light.

3.6. Identification of E1 Photoproducts

Ma *et al.* [17] found that the photochemical degradation process of E1 and E2 could produce the same by-products, which had a similar structure as E1. This suggested that the two kinds of materials had similar fates and transports in the water environment. Caupos *et al.* [25] identified E1 photoproducts by photodegradation. In the aqueous solution's absence of dissolved organic carbon (DOC), a unique photoproduct (P1, Figure 9a) was observed at a retention time higher than E1, by direct HPLC analyses. The UV-visible spectrum of P1 is identical to that of E1 and GC-MS spectra of these two compounds present the same major fragments. LC-MSⁿ experiments have been performed in positive atmospheric pressure chemical ionization (APCI) for E1 and P1. MS, MS² and MS³ spectra were identical. This set of results strongly supported the assumption that P1 was an isomer of E1. As the UV spectrum of P1 was identical to that of E1, this certainly means that the aromatic moiety remained unchanged and that structural changes were on the steroid moiety. Therefore, according to the structure of E1 and the similar characteristics of UV and mass spectra, the isomeric structure of P1 is quite difficult to put forward and the assumption that P1 corresponds to a photo enol structure should be further investigated. Trudeau *et al.* [26] researched the UV-B radiation on the photodegradation potential of estrone; UV-B-mediated degradation leads to the photoproduction of lumiestrone (Figure 9b), a little-known 13 α -epimer form of estrone.

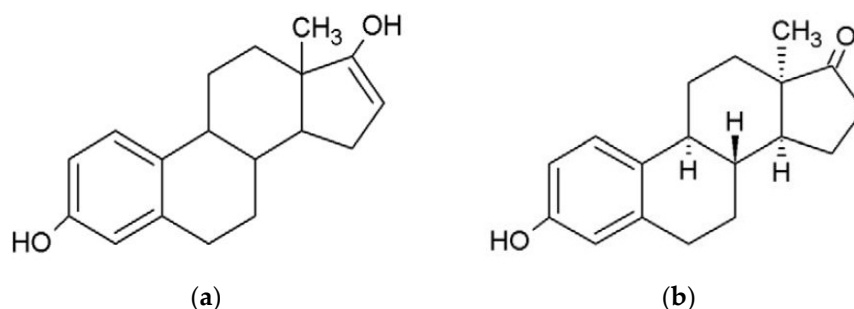


Figure 9. The possible structures of E2 and E2 degradation products: (a) P1; (b) lumiestrone.

4. Conclusions

In the study, we investigated the effects of the nano-TiO₂ content in the PVDF membrane by characterizing the composition of the prepared membranes and found that nano-TiO₂ was uniformly distributed on the membrane surface and more large pores formed in membrane surface and cross-section after adding nano-TiO₂. The PVDF-PVP-TiO₂ membrane contact angle reduced and the permeation flux increased after nano-TiO₂ was added. Compared with the rejection of E1 and E2 via PVDF-PVP membrane dynamic adsorption, and UV photolysis and PVDF-PVP membrane UV photocatalytic degradation under cross-flow conditions, we found that the use of a PVDF-PVP-TiO₂ membrane with UV had a better removal efficiency of E1 and E2; the result confirmed that the addition of nano-TiO₂ could improve estrogen degradation and adsorption under UV irradiation. The measured kinetic data of E1 and E2 removed by the PVDF-PVP-TiO₂ membrane was well described by the first-order kinetic model; the rate for the photocatalysis of E1 was 1.3 times faster than that of E2, and the addition of nano-TiO₂ in the reaction system increased the reaction rate of E2 under UV photolysis. The results indicated that the appropriate TiO₂-doped modification of the PVDF membrane could be an effective approach to improve the rejection of E1 and E2, also solving the nanometer materials' secondary environmental pollution problem in water treatments. In addition, we put a light source inside the membrane reactor, because UV irradiation is a potential trace organic removal method for TiO₂ photocatalytic membranes. This device may be able to be used in household water purifiers and rural small-scale water applications. In the future, we will continue to study the

theory of E1 and E2 removal and the service life of the TiO₂-doped PVDF membrane under ultraviolet light in depth.

Acknowledgments: This research was supported by the National Water Pollution Control and Treatment Science and Technology Major Project of China (2012ZX07404-003), Science and Technology Program for Public Wellbeing (2013GS370202-003) and Shandong Science Foundation of China (ZR2014EEQ006, ZR2014CP019, ZR2015PB010).

Author Contributions: All authors contributed to the development of this manuscript. Heng Liang, Ruibao Jia and Guibai Li conceived and designed the experiments; Mingquan Wang performed the experiments, analyzed the data and wrote the paper; Shaohua Sun contributed reagents and materials; Fangshu Qu, Heng Liang and Ruibao Jia modified the article.

Conflicts of Interest: The authors declare no conflict of interest.

References

1. Kim, S.H.; Tian, Q.; Fang, J.; Sung, S. Removal of 17- β estradiol in water by sonolysis. *Int. Biodeterior. Biodegrad.* **2015**, *102*, 11–14. [[CrossRef](#)]
2. Hanselman, T.A.; Graetz, D.A.; Wilkie, A.C. Manure-Borne estrogens as potential environmental contaminants: A review. *Environ. Sci. Technol.* **2003**, *37*, 5471–5478. [[CrossRef](#)] [[PubMed](#)]
3. Tanaka, H.; Yakou, Y.; Takahashi, A.; Higashitani, T.; Komori, K. Comparison between estrogenicities estimated from DNA recombinant yeast assay and from chemical analyses of endocrine disrupters during sewage treatment. *Environ. Sci. Technol.* **2001**, *43*, 125–132.
4. Campbell, C.G.; Borglin, S.E.; Green, F.B.; Grayson, A.; Wozei, E.; Stringfellow, W.T. Biologically directed environmental monitoring, fate, and transport of estrogenic endocrine disrupting compounds in water: A review. *Chemosphere* **2006**, *65*, 1265–1280. [[CrossRef](#)] [[PubMed](#)]
5. Kolpin, D.W.; Furlong, E.T.; Meyer, M.T.; Thurman, E.M.; Zaugg, S.D.; Barber, L.B.; Buxton, H.T. Pharmaceuticals, hormones, and other organic wastewater contaminants in US streams, 1999–2000, a national reconnaissance. *Environ. Sci. Technol.* **2002**, *36*, 1202–1211. [[CrossRef](#)] [[PubMed](#)]
6. Duong, C.N.; Ra, J.S.; Cho, J.; Kim, S.D.; Choi, H.K.; Park, J.H.; Kim, K.W.; Inam, E.; Kim, S.D. Estrogenic chemicals and estrogenicity in river waters of South Korea and seven Asian countries. *Chemosphere* **2010**, *78*, 286–293. [[CrossRef](#)] [[PubMed](#)]
7. Gong, J.; Ran, Y.; Chen, D.Y.; Yang, Y.; Ma, X.X. Occurrence and environmental risk of endocrine-disrupting chemicals in surface waters of the Pearl River, South China. *Environ. Monit. Assess.* **2009**, *156*, 199–210. [[CrossRef](#)] [[PubMed](#)]
8. Lu, P. Determination and Analysis of Environmental Endocrine Disrupting Chemicals in Trunk Stream and Tributaries of Wei-He River in Xi'an. Master's Thesis, Chang'an University, Xi'an, China, 2012.
9. Silva, C.P.; Otero, M.; Esteves, V. Processes for the elimination of estrogenic steroid hormones from water: A review. *Environ. Pollut.* **2012**, *165*, 38–58. [[CrossRef](#)] [[PubMed](#)]
10. Snyder, S.A.; Adham, S.; Redding, A.M.; Cannon, F.S.; Carolis, J.D.; Oppenheimer, J.; Wert, E.C.; Yoon, Y. Role of membranes and activated carbon in the removal of endocrine disruptors and pharmaceuticals. *Desalin* **2007**, *202*, 156–181. [[CrossRef](#)]
11. Ohko, Y.; Iuchi, K.I.; Niwa, C.; Tatsuma, T.; Nakashima, T.; Iguchi, T.; Kubota, Y.; Fujishima, A. 17 β -Estradiol Degradation by TiO₂ Photocatalysis as Means of Reducing Estrogenic Activity. *Environ. Sci. Technol.* **2002**, *36*, 4175–4181. [[CrossRef](#)] [[PubMed](#)]
12. Song, H.C.; Shao, J.H.; He, Y.L.; Liu, B.; Zhong, X.Q. Natural organic matter removal and flux decline with PEG-TiO₂-doped PVDF membranes by integration of ultrafiltration with photocatalysis. *J. Membr. Sci.* **2012**, *405–406*, 48–56. [[CrossRef](#)]
13. Song, H.C.; Shao, J.H.; Wang, J.M.; Zhong, Z.Q. The removal of natural organic matter with LiCl-TiO₂-doped PVDF membranes by integration of ultrafiltration with photocatalysis. *Desalination* **2014**, *344*, 412–421. [[CrossRef](#)]
14. Li, J.S.; Liang, Y.; Wang, H.; Sun, X.; Wang, L. Preparation and characterization of TiO₂/PVDF composite hollow fiber membrane. *Acta Polym. Sin.* **2004**, *37*, 709–712.
15. Coleman, H.M.; Routledge, E.J.; Sumpter, J.P.; Eqqins, B.R.; Byrne, J.A. Rapid loss of estrogenicity of steroid estrogens by UVA photolysis and photocatalysis over an immobilised titanium dioxide catalyst. *Water Res.* **2004**, *38*, 3233–3240. [[CrossRef](#)] [[PubMed](#)]

16. Liu, B.; Liu, X.L. Direct photolysis of estrogens in aqueous solutions. *Sci. Total Environ.* **2004**, *320*, 269–274. [[CrossRef](#)] [[PubMed](#)]
17. Ma, X.Y.; Ni, M.T.; Ni, Y.J. Competitive degradation and transformation trend of three steroid estrogens in UV system. *China Environ. Sci.* **2014**, *34*, 904–911. (In Chinese)
18. Yoon, Y.; Westerhoff, P.; Snyder, S.A.; Wert, E.C. Nanofiltration and ultrafiltration of endocrine disrupting compounds, pharmaceuticals and personal care products. *J. Membr. Sci.* **2006**, *270*, 88–100. [[CrossRef](#)]
19. Yoon, Y.; Westerhoff, P.; Snyder, S.A.; Wert, E.C.; Yoon, J. Removal of endocrine disrupting compounds and pharmaceuticals by nanofiltration and ultrafiltration membranes. *Desalination* **2007**, *202*, 16–23. [[CrossRef](#)]
20. Méricq, J.P.; Mendret, J.; Brosillon, S.; Faur, C. High performance PVDF-TiO₂ membranes for water treatment. *Chem. Eng. Sci.* **2015**, *123*, 283–291. [[CrossRef](#)]
21. Coleman, H.M.; Abdullah, M.I.; Eggins, B.R.; Palmer, F.L. Photocatalytic degradation of 17 β -estradiol, oestriol and 17 α -ethynylestradiol in water monitored using fluorescence spectroscopy. *Appl. Catal. B Environ.* **2005**, *55*, 23–30. [[CrossRef](#)]
22. Appavoo, I.A.; Hu, J.Y.; Huang, Y.; Li, S.F.Y.; Ong, S.L. Response surface modeling of Carbamazepine (CBZ) removal by Graphene-P25 nanocomposites/UVA process using central composite design. *Water Res.* **2014**, *57*, 270–279. [[CrossRef](#)] [[PubMed](#)]
23. Xiong, P.; Hu, J.Y. Degradation of acetaminophen by UVA/LED/TiO₂ process. *Sep. Purif. Technol.* **2012**, *91*, 89–95. [[CrossRef](#)]
24. Coleman, H.M.; Eggins, B.R.; Byrne, J.A.; Palmer, F.L.; King, E. Photocatalytic Degradation of 17- β -estradiol on Immobilized TiO₂. *Appl. Catal. B Environ.* **2000**, *24*, L1–L5. [[CrossRef](#)]
25. Caupos, E.; Mazellier, P.; Croue, J.P. Photodegradation of estrone enhanced by dissolved organic matter under simulated sunlight. *Water Res.* **2011**, *45*, 3341–3350. [[CrossRef](#)] [[PubMed](#)]
26. Trudeau, V.L.; Heyne, B.; Blais, J.M.; Temussi, F.; Atkinson, S.K.; Pakdel, F.; Popesku, J.T.; Marlatt, V.L.; Scaiano, J.C.; Previtiera, L.; *et al.* Lumiestrone is photochemically derived from estrone and may be released to the environment without detection. *Front. Neuroendocr.* **2011**, *2*, 83. [[CrossRef](#)] [[PubMed](#)]



© 2016 by the authors; licensee MDPI, Basel, Switzerland. This article is an open access article distributed under the terms and conditions of the Creative Commons by Attribution (CC-BY) license (<http://creativecommons.org/licenses/by/4.0/>).